High precision study of $K^{\pm} \to 3\pi^{\pm}$ decays by NA48/2

Evgueni Goudzovski*

Joint Institute for Nuclear Research, Dubna, 141980 Russia

October 21, 2006

Abstract

Preliminary results of study of $K^{\pm} \to 3\pi^{\pm}$ decays by the NA48/2 experiment at CERN SPS are presented. They include a precise measurement of the direct CP violating charge asymmetry of Dalitz plot linear slope parameters $A_g = (g^+ - g^-)/(g^+ + g^-)$, and a measurement of the Dalitz plot slope parameters (g, h, k) themselves. Due to the design of the experiment, and a large data set collected, unprecedented precisions were achieved.

Introduction

More than 40 years after its discovery [1], the phenomenon of CP violation (CPV) plays a central role in particle physics investigations. For a long time it seemed to be confined to a peculiar sector of particle physics. However, two breakthroughs took place recently. In the late 1990s, following an earlier indication by NA31 [2], the NA48 and KTeV experiments firmly established the existence of direct CPV [3, 4] by measuring a non-zero ε'/ε parameter in $K^0 \to 2\pi$ decays. In the early 2000s, a series of indirect [5] and direct [6] CPV effects in B meson decays was discovered. In kaon physics, the charge asymmetry between K^+ and K^- decays into 3π discussed here is among the most promising observables, along with the parameter ε'/ε, and rates of GIM-suppressed FCNC decays $K \to \pi\nu\bar{\nu}$.

The $K^{\pm} \to 3\pi^{\pm}$ matrix element squared is conventionally parameterized by a polynomial expansion [7]

$$|M(u,v)|^2 \sim C(u,v) \cdot (1 + gu + hu^2 + kv^2), \qquad (1)$$

where g, h, k are the linear and quadratic Dalitz plot slope parameters ($|h|, |k| \ll |g|$), $C(u,v)$ is the Coulomb factor[1], and the two kinematic vari-

*On behalf of the NA48/2 collaboration: Cambridge-CERN-Chicago-Dubna-Edinburgh-Ferrara-Firenze-Mainz-Northwestern-Perugia-Pisa-Saclay-Siegen-Torino-Wien.

[1] $C(u,v) = \prod_{i,j=1,2,3;i\neq j}\{n_{ij}/(e^{n_{ij}}-1)\}$, $n_{ij} = 2\pi\alpha e_i e_j/\beta_{ij}$, where $e_i = \pm1$ – pion charges, β_{ij} – relative velocities of pion pairs.

ables u and v are defined as

$$u = \frac{s_3 - s_0}{m_\pi^2},\ v = \frac{s_2 - s_1}{m_\pi^2},\ s_i = (P_K - P_i)^2,\ i = 1, 2, 3;\ s_0 = \frac{s_1 + s_2 + s_3}{3}. \quad (2)$$

Here m_π is the charged pion mass, P_K and P_i are the kaon and pion four-momenta, the indices $i = 1, 2$ correspond to the two identical ("even") pions and the index $i = 3$ to the other (the "odd") pion. A term proportional to v is forbidden in (1) by Bose symmetry. A difference of slope parameters g^+ and g^- describing positive and negative kaon decays, respectively, is a manifestation of direct CPV usually defined by the linear slope asymmetry

$$A_g = (g^+ - g^-)/(g^+ + g^-) \approx \Delta g/(2g), \quad (3)$$

where Δg is the slope difference and g is the average slope. The asymmetry of decay rates A_Γ is expected to be strongly suppressed with respect to A_g [8].

Several experiments had searched for the asymmetry A_g in both $\pi^\pm\pi^+\pi^-$ [9] and $\pi^\pm\pi^0\pi^0$ [10] $K^\pm$ decay modes before the NA48/2. Resulting upper limits are at the level of 10^{-3}, with large contributions of systematic uncertainties. This precision is unsatisfactory, since the SM predictions for A_g vary from a few 10^{-6} to a few 10^{-5} [11], while existing calculations involving processes beyond the SM [12] predict enhancements up to a few 10^{-4}. The primary goal of the NA48/2 experiment is A_g measurement in both decay modes with a new level of precision of 10^{-4} using a technique of simultaneous K^+/K^- beams, thus significantly reducing the gap between experiment and theory. NA48/2 $K^\pm \to 3\pi^\pm$ results obtained with partial data sample were published [13].

Precise study of $K^\pm \to 3\pi^\pm$ Dalitz plot distribution is of interest as such, since it has been recently demonstrated experimentally by study of $K^\pm \to \pi^\pm\pi^0\pi^0$ decay distribution by NA48/2 [14] and subsequently understood theoretically [15] that, due to effects of final state pion rescattering, the density of $K_{3\pi}$ Dalitz plot can be used to measure the $\pi\pi$ scattering lengths.

1 Beams and detectors

High precision measurement of A_g requires a dedicated experimental approach alongside with collection of large data samples. A novel beam line providing two simultaneous charged beams of opposite signs overlapping in space was designed and built in ECN3 high intensity hall at the CERN SPS. Allowing decays of K^+ and K^- to be recorded at the same time, it serves as a key element of the experiment, leading to cancellations of main systematic uncertainties. Regular alternation of magnetic fields in all the beam line elements was adopted to symmetrize the acceptance for the two beams. The layout of the beams and detectors is shown schematically in Fig. 1.

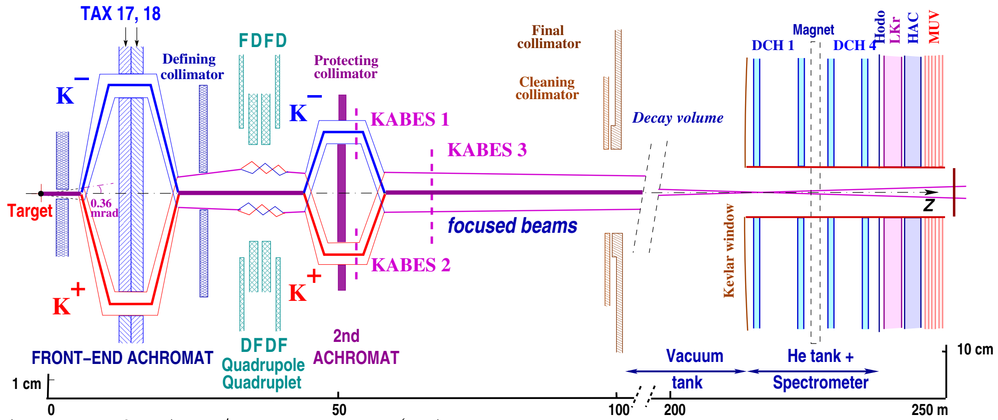

Figure 1: A view of NA48/2 beam line (TAX17,18: motorized beam dump selecting momentum of K^+/K^- beams; DFDF: focusing quadrupoles, KABES1–3: beam spectrometer) and detector (DCH1–4: drift chambers, Hodo: hodoscope, LKr: EM calorimeter, HAC: hadron calorimeter, MUV: muon veto). Vertical scale differs in two parts of the figure.

The setup is described in a right-handed coordinate system with the z axis directed downstream along the beam, and the y axis directed vertically up.

The beams are produced by 400 GeV protons impinging on a beryllium target at zero angle. Charged particles with momentum (60 ± 3) GeV/c are selected in a charge-symmetric way by an achromatic system of four dipole magnets with null total deflection, which splits the two beams in the vertical plane and recombines them on a common axis. Then the beams pass through a series of 4 quadrupoles designed to produce charge-symmetric focusing of the beams towards the detector. Finally they are again split and recombined in a second achromat housing a kaon beam spectrometer.

Further downstream both beams follow the same path. After passing the cleaning and the final collimators they enter the decay volume, housed in a 114m long cylindrical vacuum tank. With 7×10^{11} protons per burst of 4.8s duration incident on the target, the positive (negative) beam flux at the entrance of the decay volume is 3.8×10^7 (2.6×10^7) particles per pulse, of which 5.7% (4.9%) are K^+ (K^-). The K^+/K^- flux ratio is about 1.8. The fraction of beam kaons decaying in the decay volume is about 22%.

The decay volume is followed by a magnetic spectrometer used for the reconstruction of $K^\pm \to 3\pi^\pm$ decays. It is housed in a tank filled with helium at atmospheric pressure, separated from the vacuum tank by a thin $(0.31\% X_0)$ *Kevlar*-composite window. A thin-walled aluminium tube of 16 cm diameter traversing the centres of all detectors allows the undecayed beam particles to continue their path in vacuum. The spectrometer consists of 4 drift chambers (DCH): two located upstream and two downstream of the dipole magnet providing a horizontal transverse momentum kick of 120 MeV/c to the charged particles. The DCHs have a shape of a regular octagon with transverse size of about 2.8 m. Each DCH is composed of 8 planes of sense wires arranged in 4 couples of staggered planes oriented horizontally, vertically, and along each of the two orthogonal 45° directions. Momentum resolution of the spectrometer is $\sigma_p/p = 1.02\% \oplus 0.044\% p$ (p in GeV/c), corresponding to 3π invariant mass resolution of 1.7 MeV/c^2.

The spectrometer is followed by a scintillator hodoscope (HOD) consisting of a plane of horizontal and a plane of vertical strips, 64 strips arranged in 4 quadrants in each plane. A liquid krypton EM calorimeter (LKr), a hadronic calorimeter (HAC), and a muon detector (MUV) follow downstream.

The $K^\pm \rightarrow 3\pi^\pm$ decays are triggered with a two-level system. At the first level (L1), the rate of $\sim$ 500 kHz is reduced to $\sim$ 100 kHz by requiring coincidences of hits in the two HOD planes in at least two quadrants. The second level (L2) is based on a hardware system computing coordinates of DCH hits using drift times, and a farm of asynchronous microprocessors performing fast reconstruction of tracks and running the decision taking algorithm. The L2 algorithm requires at least two tracks to originate in the decay volume with the closest distance of approach of less than 5 cm. L1 triggers not satisfying this condition are examined further and accepted if there is a reconstructed track that is not compatible with a $\pi^\pm\pi^0$ decay of a $K^\pm$ having 60 GeV/c momentum directed along the z axis. The resulting trigger rate is $\sim$ 10 kHz.

NA48/2 collected data during two runs in 2003 and 2004, with $\sim$50 days of efficient data taking each. About 18×10^9 triggers were totally recorded.

2 Asymmetry measurement method

The measurement method is based on comparing the reconstructed u spectra of K^+ and K^- decays $N^+(u)$ and $N^-(u)$. Given the slope parameters values [7] and the precision of the measurement, the ratio of u spectra of $R(u) = N^+(u)/N^-(u)$ is in good approximation proportional to $(1 + \Delta g \cdot u)$, so Δg can be extracted from a linear fit to $R(u)$, and $A_g = \Delta g/2g$ can be evaluated.

Charge symmetrization of experimental conditions is to a large extent achieved by using simultaneous collinear K^+/K^- beams of similar momentum spectra. However, the presence of magnetic fields in both the beam line (achromats, quadrupoles) and the spectrometer, combined with some asymmetries in detector performance, introduces residual charge asymmetries. To equalize local effects on the acceptance, polarities of all the magnets in the beam line were reversed during the data taking on an approximately weekly basis (corresponding to the periodicity of SPS technical stops), while the polarity of the spectrometer magnet was alternated on a more frequent basis.

Data collected over a period with all the four possible setup configurations (i.e. combinations of beam line and spectrometer magnet polarities) spanning about two weeks of data taking represent a "supersample", which is treated as an independent self-consistent set of data for asymmetry measurement. Nine supersamples numbered 0 to 8 were collected in two years of running.

Each supersample contains eight distinct data samples corresponding to various combinations of setup configurations and kaon sign. In order to minimize the effects of beam and detector asymmetries, the following "quadruple ratio" involving the eight u spectra, composed as a product of four $R(u) = N^+(u)/N^-(u)$ ratios with opposite kaon sign, and deliberately chosen setup configurations in numerator and denominator, is considered:

$$R_4(u) = R_{US}(u) \cdot R_{UJ}(u) \cdot R_{DS}(u) \cdot R_{DJ}(u). \tag{4}$$

Here the indices U (D) denote beam line polarities corresponding to K^+ passing along the upper (lower) path in the achromats, and the indices S (J) represent spectrometer magnet polarities (opposite for K^+ and K^-) corresponding to the "even" pions deflection to negative (positive) x, i.e. towards the Salève (Jura) mountains. Fitting the ratio (4) with $f(u) = n\cdot(1+\Delta g\cdot u)^4$ results in two parameters: the normalization n and the slope difference Δg.

The quadruple ratio technique completes the procedure of polarity reversals, and allows a three-fold cancellation of systematic biases: 1) beam line biases cancel between K^+/K^- samples with the beams following the same path; 2) local detector biases cancel between K^+/K^- samples with decay products illuminating the same parts of the detector; 3) due to simultaneous K^+/K^- beams, global time-variable biases cancel between K^+/K^- samples.

The method is independent of the K^+/K^- flux ratio and the relative sizes of the samples collected with different setup configurations. The result remains sensitive only to time variations of asymmetries in the experimental conditions with characteristic times smaller than corresponding field alternation period, and in principle should be free of systematic biases.

With the above method, no Monte Carlo (MC) corrections to the acceptance are required. Nevertheless, a detailed GEANT-based MC simulation was developed as a tool for systematic studies, including full geometry and material description, simulation of time variations of local DCH inefficiencies, beam geometry and DCH alignment. A large MC production was made, providing a sample of a size comparable to that of the data ($\sim 10^{10}$ events).

3 Asymmetry measurement

Tracks are reconstructed from hits in DCHs using the measured magnetic field map of the spectrometer analyzing magnet rescaled according to the recorded current. Three-track vertices compatible with a $K^\pm \to 3\pi^\pm$ decay topology are reconstructed by extrapolation of track segments from the spectrometer upstream into the decay volume, taking into account the stray magnetic fields in the decay volume, and multiple scattering at the Kevlar window.

Event selection includes requirements on vertex charge, quality, and position (within the decay volume, laterally within the beam), limits on the reconstructed 3π momentum: 54 GeV/c $< P_K <$ 66 GeV/c and invariant mass: $|M_{3\pi} - M_K| < 9$ MeV/c^2 (the latter corresponding to five times the resolution). The selection leaves a practically background free sample, as $K_{3\pi}$ is the dominant three-track $K^{\pm}$ decay mode.

Fine alignment of the DCHs. Transverse positions of DCHs and individual wires were realigned every 2–4 weeks of data taking with a precision of 30μm using data collected in special runs. However, time variations of DCH alignment on a shorter time scale can potentially bias the asymmetry, since an uncorrected shift of a DCH along the x axis leads to charge-antisymmetric mismeasurement of the momenta. An unambiguous measure of the residual misalignment is the difference between the average reconstructed 3π invariant masses for K^+ and K^- decays ($\Delta\overline{M}$). Monitoring of $\Delta\overline{M}$ revealed significant (up to 200 μm) movements of the DCHs between individual alignment runs. Introduction of time-dependent corrections to the measured momenta based on the observed $\Delta\overline{M}$ reduces the effect on the slope difference by more than an order of magnitude to a negligible level of $\delta(\Delta g) < 0.1 \times 10^{-4}$.

Correction for beam geometry instabilities. The main feature determining the geometric acceptance is the beam pipe traversing the centres of DCHs. Beam optics control transverse beam positions only to ± 1 mm, leaving a sizable random charge-asymmetric bias to the acceptance. To compensate for this effect, inner radius cuts $R > 11.5$ cm are introduced for the distances of pion impact points at the first and the last DCHs from the actual average measured beam positions, at the cost of 12% of the statistics. The minimum distance of 11.5 cm is chosen to ensure that the region of the beam tube and the adjacent central insensitive areas of the DCHs are securely excluded by the cut. The average beam positions are continuously monitored separately for K^+ and K^-. In addition to the time variation of the average positions, also the dependencies of the beam position on kaon momentum are monitored and taken into account. A precision of 100 μm in the determination of beam position is sufficient to reduce systematic effects to a negligible level. Residual charge-asymmetric effects originate from permanent magnetic fields in the decay volume coupling to time-dependent DCH inefficiencies and beam migrations. The corresponding fake asymmetries do not exceed $\delta(\Delta g) = 0.2 \times 10^{-4}$.

Supersample	$K^+ \to \pi^+\pi^+\pi^-$ decays in 10^6	$K^- \to \pi^-\pi^-\pi^+$ decays in 10^6	$\Delta g \times 10^4$ raw	$\Delta g \times 10^4$ corrected
0	448.0	249.7	0.5 ± 1.4	-0.8 ± 1.8
1	270.8	150.7	-0.4 ± 1.8	-0.5 ± 1.8
2	265.5	147.8	-1.5 ± 2.0	-1.4 ± 2.0
3	86.1	48.0	0.4 ± 3.2	1.0 ± 3.3
4	232.5	129.6	-2.8 ± 1.9	-2.0 ± 2.2
5	142.4	79.4	4.7 ± 2.5	4.4 ± 2.6
6	193.8	108.0	5.1 ± 2.1	5.0 ± 2.2
7	195.9	109.1	1.7 ± 2.1	1.5 ± 2.1
8	163.9	91.4	1.3 ± 2.3	0.4 ± 2.3
Total	1998.9	1113.7	0.7 ± 0.7	0.6 ± 0.7

Table 1: Selected statistics and measured Δg in each supersample.

Trigger efficiency correction. Only charge-asymmetric inefficiencies dependent on u can bias the measurement. Inefficiencies of trigger components are measured as functions of u using control data samples from low bias triggers collected along with the main triggers, which allows to account for their time variations, and propagate their statistical errors into the result.

L1 trigger inefficiency, due to hodoscope inefficiency, was measured to be 0.9×10^{-3} and stable in time. Due to its time stability, no correction is applied, and an uncertainty of $\delta(\Delta g) = 0.3 \times 10^{-4}$, limited by the size of the control sample, is attributed. For the L2 trigger, corrections to u spectra are introduced for the rate-independent part of the inefficiency, which is time-dependent due to instabilities of the local DCH inefficiencies affecting the trigger more than the reconstruction. The integral inefficiency for the selected sample is normally close to 0.6×10^{-3}. The correction amounts to $\delta(\Delta g) = (-0.1 \pm 0.3) \times 10^{-4}$; its the error is statistical due to limited size of the control sample. The symmetry of the rate-dependent part of the inefficiency of $\sim 0.2\%$ was checked separately with MC simulation of pile-up effects.

Asymmetry fits and cross-checks. After applying the above corrections, Δg is extracted by fitting the quadruple ratio of the u spectra (4) for each supersample. Statistics selected in each supersample, the "raw" values of Δg, and the final values of Δg with the L2 trigger corrections applied are presented in Table 1. The independent results obtained in the nine supersamples are shown in Figure 2(a): they are compatible with $\chi^2/\mathrm{ndf} = 10.0/8$.

To measure sizes of the systematic biases cancelling due to the quadruple ratio technique, two other quadruple ratios of the eight u spectra were formed. These are the products of four ratios of u spectra of same sign kaons recorded with different setup configurations, therefore any physical asymmetry cancels in these ratios, while the setup asymmetries do not. The corresponding fake slope differences Δg_{LR} and Δg_{UD} in the nine supersamples are presented in

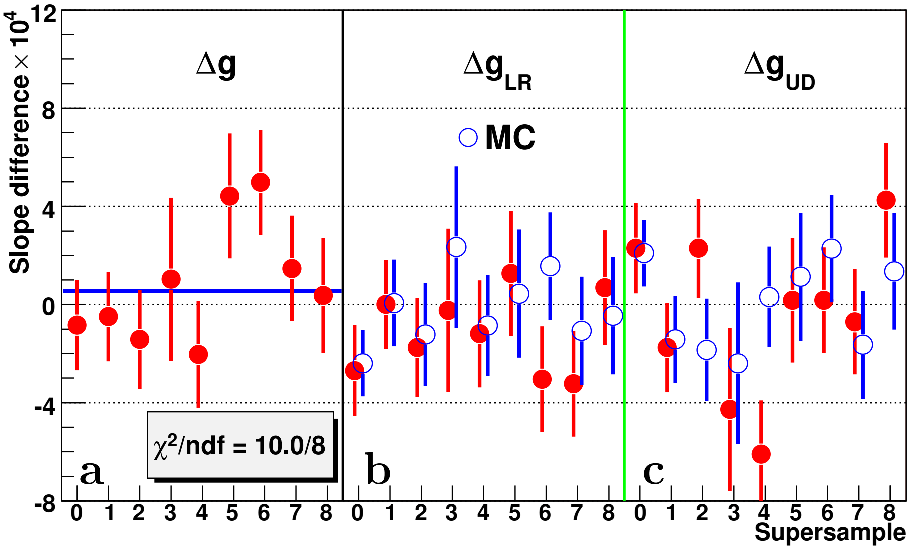

Figure 2: (a) Δg measurement in the four supersamples; control quantities (b) Δg_{LR} and (c) Δg_{UD} corresponding to detector and beam line asymmetries which cancel in quadruple ratio, and their comparison to Monte Carlo.

Figure 2(b) and (c) for both data and MC. The size of these control quantities demonstrates that the cancellation of the first-order systematic biases in (4) is at the level of a few 10^{-4}; therefore second order effects are negligible.

Limits for residual systematic effects. Pion momentum measurement is based on the knowledge of spectrometer magnet magnetic field. The precision of magnetic field reversal is 10^{-3}. Imperfect inversion effect is charge symmetric due to the simultaneous beams. An upper limit for the corresponding systematic uncertainty is $\delta(\Delta g) = 0.1 \times 10^{-4}$. In a considerable fraction of the selected events ($\sim 5\%$) a pion undergoes a $\pi \rightarrow \mu\nu$ decay in the decay volume. These events dominate the tails of the reconstructed 3π mass distribution. By varying the accepted 3π invariant mass interval in a wide range (5–25 MeV$/c^2$), a conservative systematic uncertainty of $\delta(\Delta g) = 0.4 \times 10^{-4}$ was attributed to effects due to pion decays. Effects of accidental activity and pile-up were extensively studied with MC simulation, and found to be charge-symmetric to a level of $\delta(\Delta g) = 0.2 \times 10^{-4}$, limited by MC statistics. Biases due to resolution effects were studied by varying methods of u variable calculation and binning. The result is stable within $\delta(\Delta g) = 0.3 \times 10^{-4}$. Charge-asymmetric material effects were found to be negligible. A summary of the systematic uncertainties is presented in Table 2.

4 Measurement of slope parameters

The experiment was designed for asymmetry measurements, which are MC-independent analyses relying on cancellations of systematic effects. Nevertheless, huge statistics and well tuned MC allow also precise study of $K^{\pm} \rightarrow 3\pi^{\pm}$ kinematic distribution. The ultimate goal is a full description with factoriza-

Systematic effect	Correction, uncertainty $\delta(\Delta g) \times 10^4$
Spectrometer alignment	± 0.1
Acceptance and beam geometry	± 0.2
Momentum scale	± 0.1
Pion decay	± 0.4
Pile-up	± 0.2
Resolution and fitting	± 0.3
Total systematic uncertainty	± 0.6
Level 1 trigger	± 0.3
Level 2 trigger	0.1 ± 0.3

Table 2: Systematic uncertainties and correction for level 2 trigger inefficiency.

tion of pion rescattering effects [15] and radiative corrections. However, the first stage of the analysis is interpretation in the framework of the polynomial parameterization (1), and verification of (1) at the new level of precision.

The measurement method is based on fitting the reconstructed data distribution in (u, v) with a sum of 4 MC components corresponding to the 4 terms in the polynom in (1). The relative weights of the 4 components corresponding to the best data/MC shape agreement define the values of (g, h, k). Supersamples 1–3 only are used for the preliminary analysis. Reconstruction, selection, and correction procedures are identical to those described in section 3. Uncertainties arise from spectrometer alignment and momentum scale, precision of description of DCH resolution and kaon momentum spectrum, trigger inefficiencies, and limited sizes of data and MC samples.

Validity of the parameterization (1) was demonstrated with high precision, no evidence for higher order terms was found.

Preliminary results and conclusions

The difference in $K^\pm \to 3\pi^\pm$ Dalitz plot slope parameter is found to be

$$\Delta g = g^+ - g^- = (0.6 \pm 0.7_{stat.} \pm 0.4_{trig.} \pm 0.6_{syst.}) \times 10^{-4},$$

leading to a CPV charge asymmetry using $g = -0.2154 \pm 0.0035$ [7]:

$$A_g = (-1.3 \pm 1.5_{stat.} \pm 0.9_{trig.} \pm 1.4_{syst.}) \times 10^{-4} = (-1.3 \pm 2.3) \times 10^{-4},$$

which does not contradict the SM, and due to high precision can be used to constrain SM extensions predicting enhancements of the charge asymmetry.

The following values of $K^\pm \to 3\pi^\pm$ Dalitz plot slope parameters were measured at the first stage of Dalitz plot shape analysis:

$$g = (-21.131 \pm 0.015)\%, \quad h = (1.829 \pm 0.040)\%, \quad k = (-0.467 \pm 0.012)\%.$$

They are in agreement with the world average [7] obtained by experiments made back in 1970s, but are an order of magnitude better in precision.

References

[1] J.H. Christenson *et al.*, Phys. Rev. Lett. **13** (1964) 138.

[2] H. Burkhardt *et al.* (NA31), Phys. Lett. **B206** (1988) 169.
G. Barr *et al.* (NA31), Phys. Lett. **B317** (1993) 233.

[3] V. Fanti *et al.* (NA48), Phys. Lett. **B465** (1999) 335.
A. Lai *et al.* (NA48), Eur. Phys. J. **C22** (2001) 231.
J.R. Batley *et al.* (NA48), Phys. Lett. **B544** (2002) 97.

[4] A. Alavi-Harati *et al.* (KTeV), Phys. Rev. Lett. **83** (1999) 22.
A. Alavi-Harati *et al.* (KTeV), Phys. Rev. **D67** (2003) 012005.

[5] B. Aubert *et al.* (Babar), Phys. Rev. Lett. **87** (2001) 091801.
K. Abe *et al.* (Belle), Phys. Rev. Lett. **87** (2001) 091802.

[6] K. Abe *et al.* (Belle), Phys. Rev. Lett. **93** (2004) 021601.
B. Aubert *et al.* (Babar), Phys. Rev. Lett. **93** (2004) 131801.

[7] W.-M. Yao *et al.* (PDG), J. Phys. **G33** (2006) 1.

[8] G. Isidori, L. Maiani, A. Pugliese, Nucl. Phys. **B381** (1992) 522.

[9] W.T. Ford *et al.*, Phys. Rev. Lett. **25** (1970) 1370.

[10] K.M. Smith *et al.*, Nucl. Phys. **B91** (1975) 45.
G.A. Akopdzhanov *et al.* (TNF–IHEP), Eur. Phys. J. **C40** (2005) 343.

[11] G. Fäldt and E.P. Shabalin, Phys. Lett. **B635** (2006) 295.
A.A. Belkov, A.V. Lanyov, G. Bohm, Czech. J. Phys. **55B** (2004) 193.
E. Gamiz, J. Prades, I. Scimemi, JHEP **0310** (2003) 042.
G. D'Ambrosio, G. Isidori, Int. J. Mod. Phys. **A13** (1998) 1.

[12] G. D'Ambrosio, G. Isidori, G. Martinelli, Phys. Lett. **B480** (2000) 164.
E.P. Shabalin, ITEP preprint **8-98** (1998).

[13] J.R. Batley *et al.* (NA48/2), Phys. Lett. **B634** (2006) 474.

[14] J. R. Batley *et al.* (NA48/2), Phys. Lett. **B633** (2006) 173.
M. Pepe, these proceedings.

[15] N. Cabibbo, G. Isidori, JHEP **503** (2005) 21.